RAA 2020 Vol. **20** No. **9**, 139(9pp) doi: 10.1088/1674–4527/20/9/139

http://www.raa-journal.org *http://iopscience.iop.org/raa*

***R**esearch in*
***A**stronomy and*
***A**strophysics*

Statistical relations between stellar spectral and luminosity classes and stellar effective temperature and surface gravity

Oleg Malkov[1,2], Dana Kovaleva[2], Sergey Sichevsky[2] and Gang Zhao[1]

[1] Key Laboratory of Optical Astronomy, National Astronomical Observatories, Chinese Academy of Sciences, Beijing 100012, China; *malkov@inasan.ru*
[2] Institute of Astronomy, Russian Academy of Sciences, 48 Pyatnitskaya St., Moscow 119017, Russia

Received 2020 January 22; accepted 2020 April 8

Abstract We have determined new statistical relations to estimate the fundamental atmospheric parameters of effective temperature and surface gravity, using MK spectral classification, and vice versa. The relations were constructed based on the published calibration tables (for main sequence stars) and observational data from stellar spectral atlases (for giants and supergiants). These new relations were applied to field giants with known atmospheric parameters, and the results of the comparison of our estimations with available spectral classification have been quite satisfactory.

Key words: stars: fundamental parameters

1 INTRODUCTION

Knowledge of the average effective temperature ($T_{\rm eff}$) or surface gravity ($\log g$) of a star of given spectral class and luminosity class is often needed to solve various problems in astrophysics. In particular, in the course of our investigation on interstellar extinction and parameterization of stars, the necessity was felt to have general statistical relations between the semi-quantitative parameters spectral class and luminosity class on the one hand, and $T_{\rm eff}$ and $\log g$ on the other hand. In our study we consider photometry from modern large sky surveys (DENIS, 2MASS, SDSS, GALEX, UKIDSS, WISE, IPHAS, Pan-STARRS), containing photometric (3 to 5 bands) data for $10^7 - 10^9$ stars. We cross-match objects in these surveys and can then estimate spectral classes, luminosity classes, distances (d) and interstellar extinction values (A_V), minimizing the function

$$\chi^2 = \sum_{i=1}^{N} \left(\frac{m_{{\rm obs},i} - m_{{\rm calc},i}}{\sigma m_{{\rm obs},i}} \right)^2 , \qquad (1)$$

where $m_{{\rm obs},i}$ and $\sigma m_{{\rm obs},i}$ are the apparent magnitude and its observational error, respectively, in the i-th photometric band from a given survey, and the summation is over up to $N \sim 30$ photometric bands, and

$$m_{{\rm calc},i} = M_i + 5 \log d - 5 + A_i . \qquad (2)$$

Here $A_i = f(A_V)$ is the extinction in the i-th photometric band, and can be determined from the interstellar extinction law. The procedure and pilot results (including their comparison with recent Gaia Data Release 2 (DR2) parallaxes) are described in detail in Malkov et al. (2010), Sichevskiy et al. (2013), Sichevskij et al. (2014), Malkov et al. (2018a) and Malkov et al. (2018b).

$M_i = f({\rm spectralclass}, {\rm luminosityclass})$ is the absolute magnitude in the i-th photometric band taken from calibration tables. To obtain absolute magnitudes for stars of different spectral classes and luminosity classes in the corresponding photometric systems M_i, we referenced tables of absolute magnitudes in 2MASS, SDSS and GALEX systems (Kraus & Hillenbrand 2007; Findeisen et al. 2011). However, corresponding calibration tables, which provide stellar absolute magnitudes in a given photometric system for all spectral classes, cannot be found in the literature for UKIDSS and other surveys. In the absence of such information, it is necessary to construct corresponding relations from theoretical spectral energy distributions (SEDs) and photometric system response curves. The best source for theoretical SEDs is libraries of synthetic spectra (Lejeune et al. 1997; Castelli & Kurucz 2003; Gustafsson et al. 2008), and the SEDs are computed there for a given set of atmospheric parameters ($\log T_{\rm eff}$, $\log g$, metallicity) rather than spectral classes. Thus, for the solution of this problem, it is necessary to design relations between spectral class and atmospheric parameters, for different luminosity classes. In

other words, we have faced questions like, e.g., what are the values of $T_{\rm eff}$ and $\log g$ for an A2V type star?

Several methods were developed to estimate atmospheric parameters of effective temperature ($T_{\rm eff}$) and surface gravity ($\log g$), using photometric indices in the $uvby$ (Kim & Moon 2011), $BVRIJHK$ (Kim & Moon 2014) and other colour systems. On the other hand, several calibration tables, connecting MK spectral classification with colour indices in $ugriz$ (Covey et al. 2007; Kraus & Hillenbrand 2007), GALEX FUV/NUV (Findeisen & Hillenbrand 2010; Findeisen et al. 2011), JHK (Pecaut & Mamajek 2013) and other photometric systems, were published. However, there is a lack of relations between MK spectral classification and atmospheric parameters. Individual precise measurements of fundamental parameters of $T_{\rm eff}$ and $\log g$ are published in many sources, however, they are presented mostly for main sequence (MS) stars (see, e.g., Smalley & Dworetsky 1995).

The goal of this study is to construct analytical statistical relations between MK spectral class and the atmospheric parameters ($T_{\rm eff}$, $\log g$) for principal luminosity classes. Similar work was done more than thirty years ago by de Jager & Nieuwenhuijzen (1987), where statistical relations between stellar spectral and luminosity classes and stellar effective temperature and luminosity (but not surface gravity) were determined. Several authors published interpolation tables presenting ($T_{\rm eff}$, $\log g$) – (spectral class, luminosity class) relations (see Sect. 2 for references), but we wanted to add more recent determinations of $T_{\rm eff}$ and $\log g$ to these data. Also, it appeared necessary to have these relations adapted for computer-use, which would enhance their usefulness.

The paper is organised as follows. Observational data and published relations used in the present study are listed in and briefly discussed in Section 2. Construction of (spectral class — $\log T_{\rm eff}/\log g$) statistical relations for dwarfs, supergiants and giants is described in Sections 3.1, 3.2 and 3.3, respectively. Application of these relations to stars with known metallicity is discussed in Section 4. Section 5 contains verification of our results with Large Sky Area Multi-Object Fiber Spectroscopic Telescope (LAMOST) data, and we draw our conclusions in Section 6.

2 DATA SOURCES

The main source of accurate data on stellar astrophysical parameters is components of detached double-lined eclipsing binaries. The lists of such binaries were compiled by Popper (1980), Harmanec (1988), Andersen (1991), Torres et al. (2010) and Eker et al. (2018), and they contain mostly MS stars.

Another useful source of stars with available spectral classification and known atmospheric parameters is empirical stellar spectral atlases. In the current study, we consider data from ELODIE (Prugniel et al. 2007), Indo-US (Valdes et al. 2004), MILES (Falcón-Barroso et al. 2011) and STELIB (Le Borgne et al. 2003) libraries.

Calibration tables based on observational data were constructed by Johnson (1966), Allen (1976), Popper (1980), Straižys (1992), Pecaut & Mamajek (2013) (see also Mamajek's data available at `http://www.pas.rochester.edu/~emamajek/EEM_dwarf_UBVIJHK_colors_Teff.txt` and published in Pecaut et al. 2012) and Eker et al. (2018). Of these, only Allen (1976) and Straižys (1992) presented $\log g$ values for non-MS stars.

3 CONSTRUCTION OF STATISTICAL RELATIONS

3.1 Main Sequence Stars

To construct an analytic (spectral class – atmospheric parameters) formula for MS stars, we have employed published relations and applied a polynomial approximation.

Spectral class — effective temperature relations of different authors demonstrate excellent agreement (see Fig. 1). To draw an analytical form for the spectral class — $\log T_{\rm eff}$ relation we have used Eker et al. (2018) data, with Pecaut & Mamajek (2013) extension to the coolest stars.

An agreement of (spectral class — surface gravity) relations for the same authors is worse (see Fig. 1). To construct the (spectral class — $\log g$) analytic formula we have utilised all three relations.

The results are presented in Table 1 (Eqs. (T1-T4)) and Figure 1.

3.2 Supergiants

Supergiants are rare in the Galaxy but due to high intrinsic luminosity they are relatively numerous in observational catalogues and surveys, especially at low Galactic latitudes. In particular, 276 of 9110 stars in the Bright Star Catalogue (Hoffleit & Jaschek 1991) are supergiants.

To construct an analytic (spectral class – atmospheric parameters) formula for supergiant stars, we have used data from the empirical stellar spectral atlases ELODIE (Prugniel et al. 2007), Indo-US (Valdes et al. 2004), MILES (Falcón-Barroso et al. 2011) and STELIB (Le Borgne et al. 2003), and made a polynomial approximation.

Approximating the observational data, we do not separate high (Ia), intermediate (Iab) and low (Ib) luminosi-

Table 1 Spectral Class — Effective Temperature — Surface Gravity Relations

			std. dev.	valid for	Eq.
LC=V					
$\log T_{\rm eff}$	=	$4.80223 - 0.0465961S + 0.00157054S^2$	0.004	O3–O9	(T1)
$\log T_{\rm eff}$	=	$5.30408 - 0.111312S + 0.00284209S^2 - 2.51285e^{-5}S^3$	0.011	B0–G7	
$\log T_{\rm eff}$	=	$3.25745 + 0.0285452S - 0.000388153S^2$	0.008	G8–M9	
S	=	$-77.4025 - 208.506T - 72.7616T^2$	0.36	$3.38 \le \log T_{\rm eff} < 3.75$	(T2)
S	=	$13.0566 + 68.6827T + 404.486T^2 + 751.011T^3 + 497.913T^4$	0.75	$3.75 \le \log T_{\rm eff} < 4.10$	
S	=	$5.53554 - 34.2627T - 4.78570T^2 + 191.168T^3 + 317.065T^4$	0.34	$4.10 \le \log T_{\rm eff} \le 4.72$	
$\log g$	=	$4.23248 + 0.0194541S_1 + 0.000552749S_1^2 - 4.30515e^{-5}S_1^3 - -1.09920e^{-6}S_1^4 + 7.61843e^{-8}S_1^5 + 8.20985e^{-10}S_1^6 - 3.27874e^{-11}S_1^7$	0.055	O3–M9.5	(T3)
S	=	$-0.117642 + 1.07059G + 192.069G^2 - 183.386G^3 + 49.7143G^4$	4.02	$3.8 \le \log g \le 5.3$	(T4)
LC=I					
$\log T_{\rm eff}$	=	$5.37107 - 0.132197S + 0.00447197S^2 - 7.12416e^{-5}S^3 + 4.17523e^{-7}S^4$	0.049	O7–M3	(T5)
S	=	$5.87386 - 49.0805T - 135.952T^2 - 119.090T^3 + 124.459T^4 + 108.708T^5$	3.14	$3.45 \le \log T_{\rm eff} < 4.60$	(T6)
$\log g$	=	$5.26666 - 0.289286S + 0.00728099S^2 - 6.33673e^{-5}S^3$	0.485	O7–M3	(T7)
S	=	$5.26199 - 10.2492G + 2.79561G^2 + 0.526251G^3$	9.74	$-0.2 \le \log g \le 3.8$	(T8)
LC=III					
$\log T_{\rm eff}$	=	$5.07073 - 0.0757056S + 0.00147089S^2 - 1.03905e^{-5}S^3$	0.034	O5–M10	(T9)
S	=	$8.49594 - 49.4053T - 191.524T^2 - 335.488T^3 - 144.781T^4$	2.59	$3.45 \le \log T_{\rm eff} < 4.65$	(T10)
$\log g$	=	$3.79253 - 0.0136260S + 0.000562512S^2 - 1.68363e^{-5}S^3$	0.513	O5–M10	(T11)
S	=	$33.3474 - 18.3022G - 5.33024G^2 - 0.667234G^3$	7.03	$-0.5 \le \log g \le 4.7$	(T12)

S is spectral class code: 3 for O3, ..., 10 for B0, ..., 60 for M0; $S_1 = S - 35$; $T = \log T_{\rm eff} - 4.6$; $G = \log g - 3.7$.

ty supergiant stars, and construct overall relations for all supergiants. Empirical stellar spectral libraries do not provide observational errors for atmospheric parameters, so we have assigned equal weight to all stars.

The results are presented in Table 1 (Eqs. (T5-T8)) and Figure 2.

3.3 Giants

As in the previous section, to construct an analytic (spectral class – atmospheric parameters) formula for giant stars, we have incorporated data from the empirical stellar spectral atlases ELODIE (Prugniel et al. 2007), Indo-US (Valdes et al. 2004), MILES (Falcón-Barroso et al. 2011) and STELIB (Le Borgne et al. 2003) (besides that, a small number of giants from the Eker et al. (2018) list was added) and implemented a polynomial approximation.

The results are presented in Table 1 (Eqs. (T9-T12)) and Figure 3.

4 STARS WITH KNOWN METALLICITY

Spectral classification (in contrast to narrow band photometry) is a very poor indicator of stellar metallicity [Fe/H]. Also, the number of stars with known chemical abundance is much less than the number of stars with available spectral classification and/or $\log T_{\rm eff}$ / $\log g$ parameters. Last but not least, there is no obvious correlation between the initial mass (i.e., spectral class) of a star and its metallicity.

Equations in Table 1 are derived assuming one does not have data on stellar metallicity. However, sometimes data on [Fe/H] are available, along with data on $T_{\rm eff}$ and $\log g$. In this case, some corrections can be made to those equations.

To calculate these corrections, we have selected giant and supergiant stars with known spectral class, effective temperature $T_{\rm eff}$, surface gravity $\log g$ and metallicity [Fe/H] from the empirical stellar spectral atlases ELODIE (Prugniel et al. 2007), Indo-US (Valdes et al. 2004), MILES (Falcón-Barroso et al. 2011) and STELIB (Le Borgne et al. 2003). Besides, three giants from Torres et al. (2010) were added.

After a preliminary analysis, some stars were removed from the list. The following giant stars were excluded from consideration:

- HD 216131=μ Peg has $T_{\rm eff}$=4950 K, which is a little hotter than what is required for M2III (ELODIE), however, it is perfectly consistent with G8III (Indo-US, MILES).
- HD 130322 seems too dense ($\log g$=4.54) for its spectral class K0III (ELODIE). According to SIMBAD, its spectral class is K0V.
- Conversely, HD 37202 seems too rarefied ($\log g$=2.47) for its spectral class B4IIIp (ELODIE). Indeed, ac-

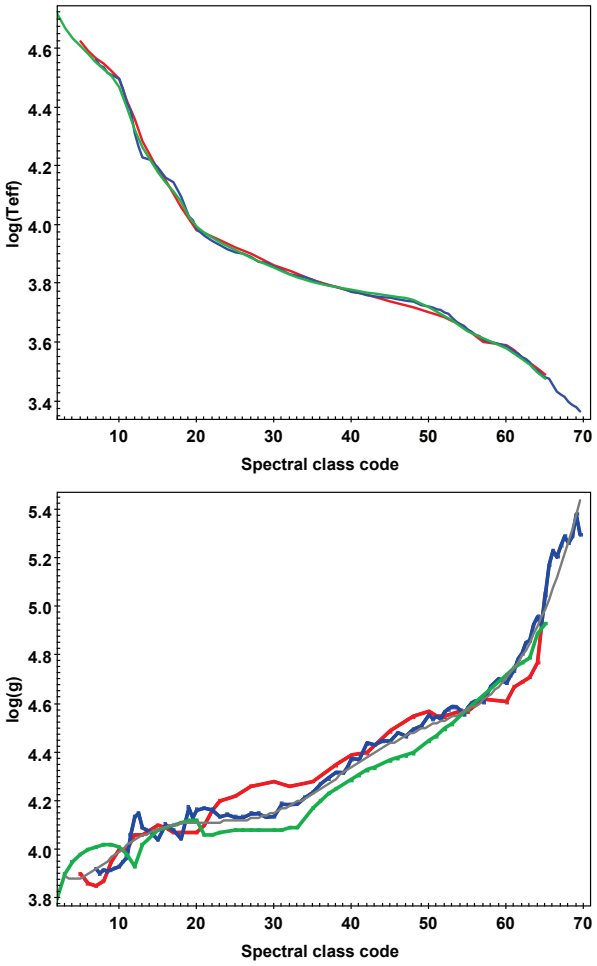

Fig. 1 MS stars. Spectral class — effective temperature (*top panel*) and spectral class — surface gravity (*bottom panel*) relations. Spectral class is coded as follows: 3 for O3, ..., 10 for B0, ..., 60 for M0. Straižys (1992), Pecaut & Mamajek (2013) and Eker et al. (2018) data are represented by red, blue and green curves, respectively. The gray curve is the (log g – spectral class) relation, approximated by a polynomial (see Table 1, Eq. (T3)).

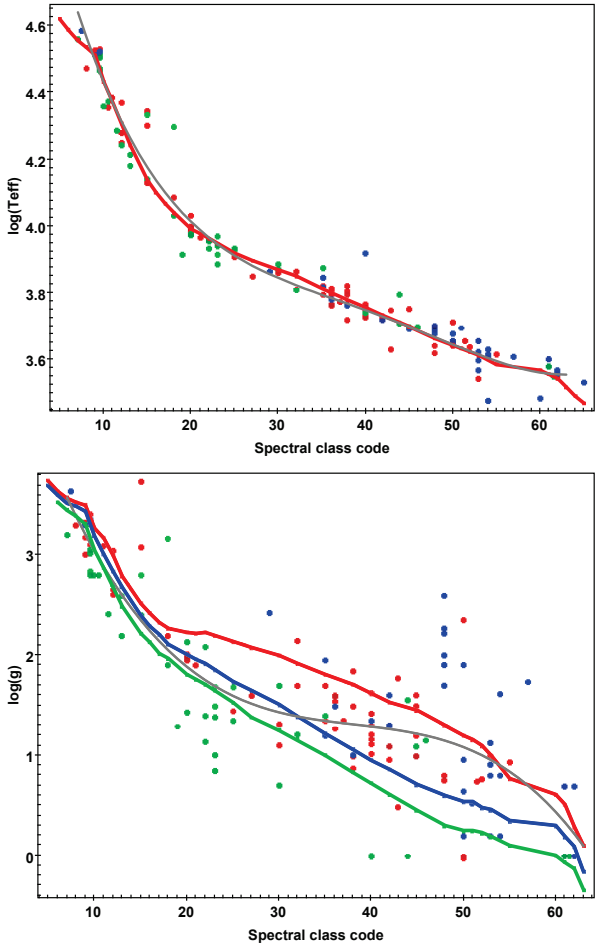

Fig. 2 Supergiants. Spectral class — effective temperature (*top panel*) and spectral class — surface gravity (*bottom panel*) relations. Spectral class is coded as follows: 3 for O3, ..., 10 for B0, ..., 60 for M0. Low (Ib), intermediate (Iab) and high (Ia) luminosity supergiants, selected from empirical stellar spectral atlases, are represented by red, blue and green dots, respectively. Gray curves are the ($\log T_{\rm eff}$ – spectral class) and (log g – spectral class) relations, approximated by a polynomial (see Table 1, Eqs. (T5) and (T7), respectively). *Top panel*: red curve represents Straižys (1992) (spectral class – $\log T_{\rm eff}$) relation for supergiants. *Bottom panel*: green, blue and red curves signify Straižys (1992) (spectral class – $\log g$) relations for Ia, Iab and Ib supergiants, respectively.

cording to the General Catalogue of Stellar Spectral Classifications (Skiff 2014), it belongs to the bright giant sequence and has spectral class B3IIp.

– The same can be said for HD 190390. According to SIMBAD, its spectral class is F2II, which is more consistent with surface gravity value $\log g$=1.25 than F1III (Indo-US).
– Besides, we have excluded HD 196777=υ Cap, a variable star, which looks too hot ($T_{\rm eff}$=10 500 K) and too dense ($\log g$=4.00) for its spectral class M1III (Indo-US).

Also, we have excluded some supergiants from further consideration.

– $T_{\rm eff}$ of HD 217476 is 8320 K, which seems too large for G0Iab (ELODIE). The values listed in MILES look more self-consistent (G4Ia, $T_{\rm eff}$=5100 K).
– Spectral class G4Ia of HD 6474 seems too late for its $T_{\rm eff}$=6240 K (MILES), while General Catalogue of Stellar Spectral Classifications (Skiff 2014) lists spectral classes from F8Ia to G5 for this star.
– Spectral class K0Iab is catalogued for HD 104893, but, according to SIMBAD, its spectral class is F8/G2.

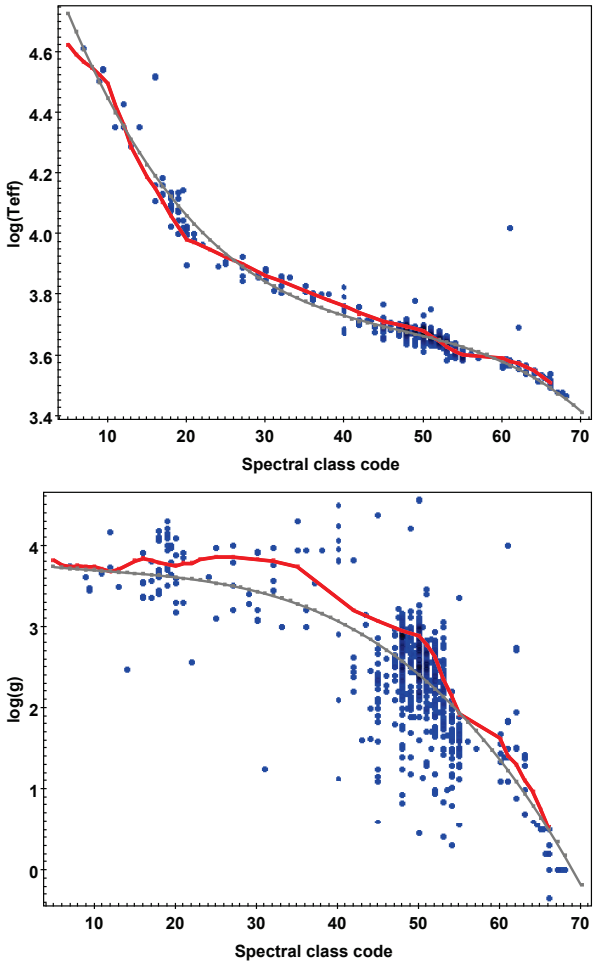

Fig. 3 Giants. Spectral class — effective temperature (*top panel*) and spectral class — surface gravity (*bottom panel*) relations. Spectral class is coded as follows: 3 for O3, ..., 10 for B0, ..., 60 for M0. Dots represent giants, selected from empirical stellar spectral atlases. Gray curves are the ($\log T_{\rm eff}$ – spectral class) and ($\log$ g – spectral class) relations, approximated by a polynomial (see Table 1, Eqs. (T9) and (T11), respectively). Red curves represent Straižys (1992) (spectral class – $\log T_{\rm eff}$) and (spectral class – $\log g$) relations for giants.

For the remaining 783 giants and 122 supergiants (their [Fe/H] distributions are displayed in Fig. 4), we have computed spectral classes from $T_{\rm eff}$ and $\log g$ with Equations (T10) and (T12) for giants, and with Equations (T6) and (T8) for supergiants. The resulting values, SpT($T_{\rm eff}$) and SpT($\log g$), were compared with spectral classes SpT$_{\rm cat}$, catalogued in the atlases. The difference, expressed as observed minus computed ($O-C$) spectral class, is shown in Figures 5 and 6 as a function of metallicity. The Y-axis in Figures 5 and 6 is graded so that one unit corresponds to one spectral sub-class (e.g., the difference between A1 and A2).

One can see that the difference between observed minus computed spectral class correlates with metallicity. For

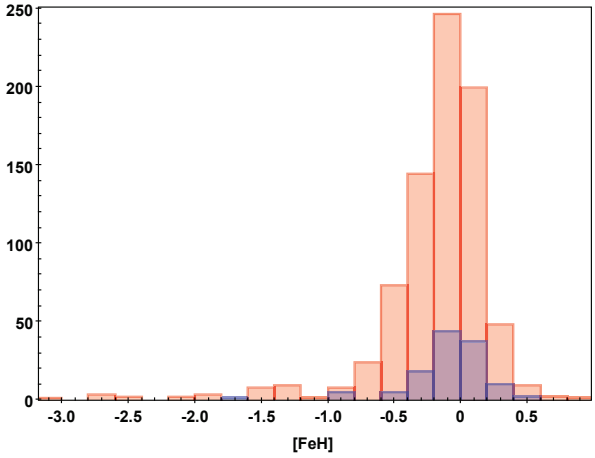

Fig. 4 Metallicity distribution of 783 giants (*red bars*) and 122 supergiants (*blue bars*). Stars are from ELODIE, MILES, Indo-US, STELIB empirical stellar spectral atlases and from the Torres et al. (2010) list.

giant stars, the spectral class value, computed from $T_{\rm eff}$ with Equation (T10), should be increased by the value of $\Delta SpT(T)$, where the

$$\Delta SpT(T) \equiv SpT_{\rm cat} - SpT(T_{\rm eff}) = 2.04[{\rm Fe/H}] - 0.34, \quad (3)$$

correlation coefficient is 0.44 (see Fig. 5, upper panel). Here SpT$_{\rm cat}$ is the spectral class, catalogued in the empirical stellar spectral atlases, and SpT($T_{\rm eff}$) is the spectral class, calculated from $T_{\rm eff}$ with Equation (T10).

Similar to Equation (3), the spectral class value, computed from $\log g$ with Equation (T12), should be increased by the value of $\Delta SpT(G)$, where the

$$\Delta SpT(G) \equiv SpT_{\rm cat} - SpT(\log g) = 3.84[{\rm Fe/H}] + 0.73, \quad (4)$$

correlation coefficient is 0.26 (see Fig. 5, lower panel). Here SpT$_{\rm cat}$ is the spectral class, catalogued in the empirical stellar spectral atlases, and SpT($\log g$) is the spectral class, calculated from $\log g$ with Equation (T12). Note that the standard deviation of $\Delta SpT(G)$ (std.dev.=6.2) is much larger than the one of $\Delta SpT(T)$ (std.dev.=1.9). Equations (3) and (4) are valid for $-3 \le [{\rm Fe/H}] \le 0.85$

The analogous relations for supergiants are not so obvious. The following conclusions can be drawn from Figure 6 (top panel)

$$\Delta SpT(T) \equiv SpT_{\rm cat} - SpT(T_{\rm eff}) = \begin{cases} 0, & \text{for } -0.42 \le [{\rm Fe/H}] \le 0.48; \\ -1.6, & \text{for } -0.9 \le [{\rm Fe/H}] \le -0.8. \end{cases} \quad (5)$$

Here SpT($T_{\rm eff}$) is the spectral class, calculated from $T_{\rm eff}$ with Equation (T6).

The lack of data does not allow us to draw definite conclusions beyond these ranges. In particular, the data on the

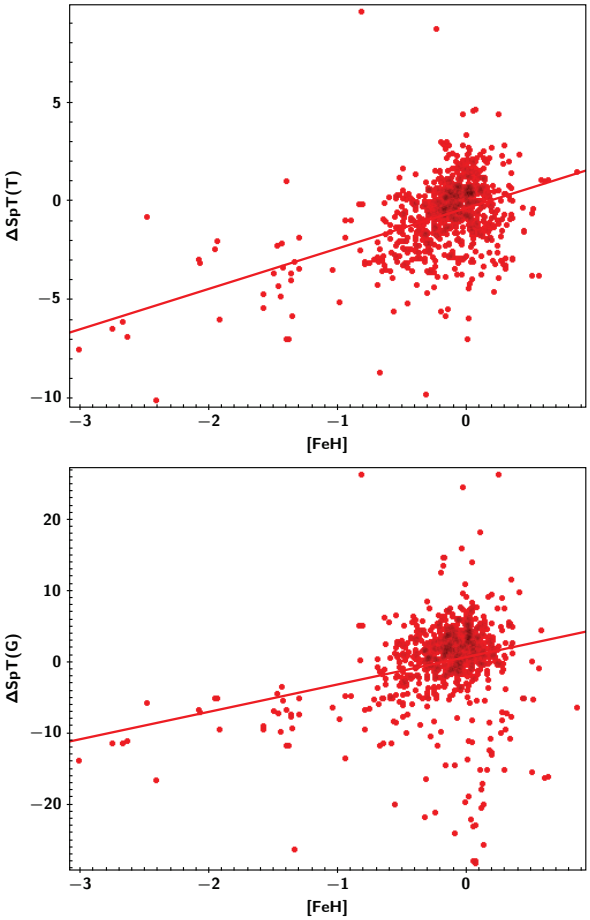

Fig. 5 Giants. Difference between observed minus computed spectral class vs. metallicity. *Top panel*: $\Delta SpT(T) = SpT_{\rm cat} - SpT(T_{\rm eff})$, where $\mathrm{SpT}_{\rm cat}$ is the spectral class, catalogued in the empirical stellar spectral atlases, and $\mathrm{SpT}(T_{\rm eff})$ is the spectral class, calculated from $T_{\rm eff}$ with Eq. (T10). *Bottom panel*: $\Delta SpT(G) = SpT_{\rm cat} - SpT(\log g)$, where $\mathrm{SpT}(\log g)$ is the spectral class, calculated from $\log g$ with Eq. (T12). Linear fit is traced by the solid line. The Y-axis is graded so that one unit corresponds to one spectral sub-class (e.g., the difference between A1 and A2).

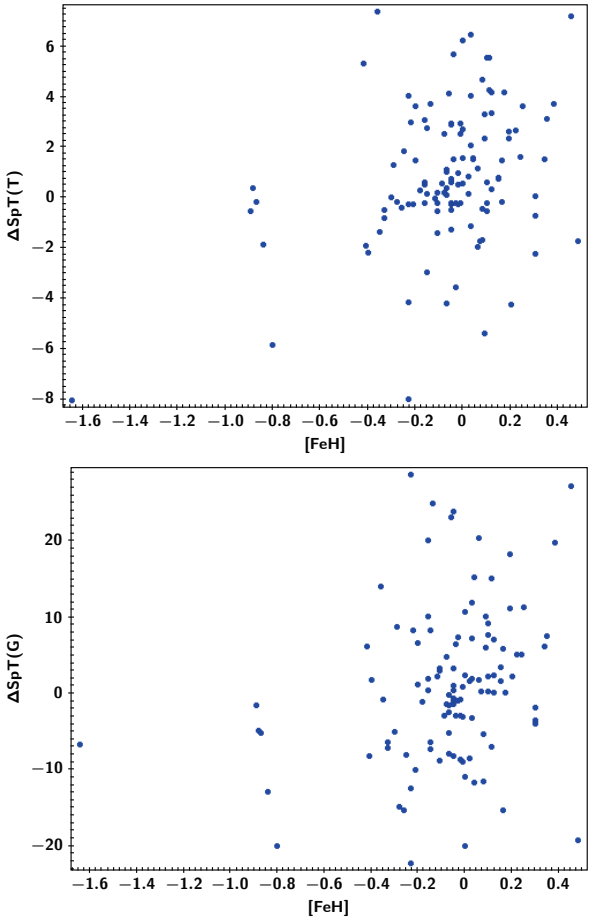

Fig. 6 Supergiants. Difference between observed minus computed spectral class vs. metallicity. *Top panel*: $\Delta SpT(T) = SpT_{\rm cat} - SpT(T_{\rm eff})$, where $\mathrm{SpT}_{\rm cat}$ is the spectral class, catalogued in the empirical stellar spectral atlases, and $\mathrm{SpT}(T_{\rm eff})$ is the spectral class, calculated from $T_{\rm eff}$ with Eq. (T6). *Bottom panel*: $\Delta SpT(G) = SpT_{\rm cat} - SpT(\log g)$, where $\mathrm{SpT}(\log g)$ is the spectral class, calculated from $\log g$ with Eq. (T8). The Y-axis is graded so that one unit corresponds to one spectral subclass (e.g., the difference between A1 and A2).

lowest metallicity stars are too scarce to make conclusions: the only supergiant star with lower metallicity in our sample, HD 103036 = TY Vir ([Fe/H]=-1.64), is a long-period semiregular variable star.

The large standard deviation of $\Delta SpT(G)$ (std.dev.=9.8, see Fig. 6, lower panel) indicates that Equation (T8) should be applied with caution, and only in the range $-0.42 \leq [\mathrm{Fe/H}] \leq 0.48$ (where $\Delta SpT(G)$=0 can be used, as a first approximation).

5 VERIFICATION OF RESULTS WITH LAMOST DATA

To verify our results, we have employed data from LAMOST, the largest source, containing independently determined spectral classes and atmospheric parameters for tens of thousands of stars.

LAMOST is a special reflecting Schmidt telescope (Cui et al. 2012), which can observe 4000 spectra simultaneously in a single exposure. Consequently, LAMOST has great potential to efficiently survey a large volume of space for stars and galaxies (Zhao et al. 2012).

The LAMOST AFGK star catalogue (Luo et al. 2015) contains 5 843 107 objects (Data Release 6 (DR6) V1). Atmospheric parameters and spectral classes are determined for them, and part of the objects also have luminosity classes. The LAMOST stellar spectral classification procedure is described by Wei et al. (2014).

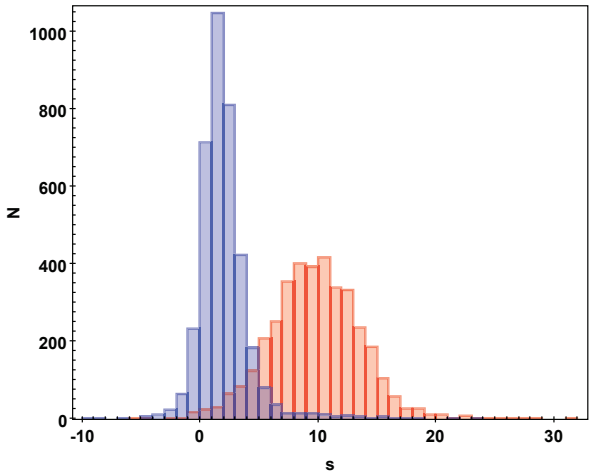

Fig. 7 Comparison of our results for LAMOST giant stars. The red histogram is the $s_t - s_g$ distribution, and the blue histogram is the $\bar{s} - s_{LAMOST}$ distribution. See Sect. 5 for details.

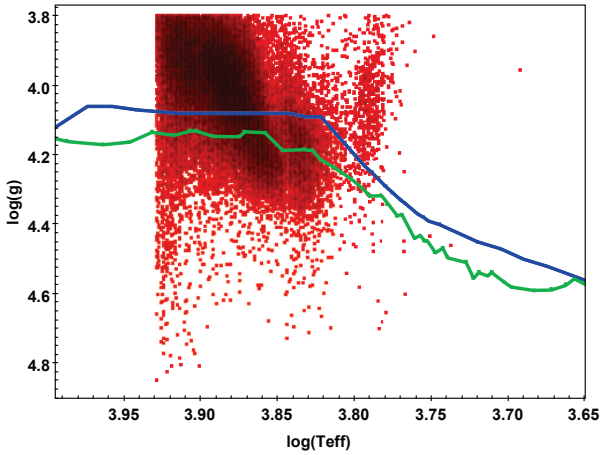

Fig. 8 LAMOST DR6 MS stars on the $\log T_{\rm eff} - \log g$ plot (*red dots*). Blue and green curves represent corresponding relations by Eker et al. (2018) and Pecaut & Mamajek (2013), respectively. Note that the X- and Y-axes are flipped.

MS, giant and subgiant stars are included in the LAMOST classification scheme. Supergiants are not indicated in the LAMOST catalogue.

5.1 Giants

Among 5 843 107 catalogued objects, 3716 stars are classified as (mostly late-A) giants. For those stars, we have estimated spectral classes independently from $T_{\rm eff}$ and $\log g$ values from the catalogue (applying Eqs. (T10) and (T12) from Table 1, respectively), and compared them with catalogued spectral classes.

The result of our comparison for those 3716 stars is summarised in Figure 7. We have calculated a difference $s_t - s_g$, where s_t and s_g represent spectral class code estimated from effective temperature (Table 1, Eq. (T10)) and surface gravity (Table 1, Eq. (T12)), respectively. Again, here spectral class is coded as follows: 3 for O3, ..., 10 for B0, ..., 60 for M0. We have also calculated an average value $\bar{s} = (s_t + s_g)/2$ and compared this value with catalogued spectral class $s_{\rm LAMOST}$. The red histogram in Figure 7 is the $s_t - s_g$ distribution, and the blue histogram is the $\bar{s} - s_{\rm LAMOST}$ distribution. One can see that whereas s_t is consistently about one class later than s_g, the average value $\bar{s}$, estimated from effective temperature and surface gravity, in most cases differs by not more than three spectral sub-classes from the catalogued spectral class $s_{\rm LAMOST}$. For 78% and 90% of stars, that difference does not exceed three and four spectral sub-classes, respectively (see the blue histogram in Fig. 7). Mean value for the difference $\bar{s} - s_{\rm LAMOST}$ is 1.99. It means that, e.g., for an A7III star, our procedure predicts, on average, A9III spectral class.

5.2 Main Sequence Stars

The LAMOST DR6 AFGK catalogue contains 63 220 stars marked as having luminosity class V. Part of them have $\log g < 3.8$ (up to $\log g = 0.784$), which is beyond the applicability of Eq. (T4) (see Table 1), and they have been excluded from further analysis. All of the remaining 58 652 stars have spectral class A, and 90% of them belong to A5 or A7 sub-class.

The spread of these stars on the $\log T_{\rm eff} - \log g$ plot is depicted in Figure 8, together with corresponding relations by Eker et al. (2018) and Pecaut & Mamajek (2013). Note that according to the Eker et al. (2018) and Pecaut & Mamajek (2013) relations, the range of A-stars is limited to approximately the following values, $4.00 \geq \log T_{\rm eff} \geq 3.87$ and $4.0 \leq \log g \leq 4.2$. It can be seen that some of the LAMOST stars are located far (sometimes quite far) beyond this range.

For those 58 652 MS stars, we have estimated spectral classes independently from $T_{\rm eff}$ and $\log g$ values from the catalogue (using Eqs. (T2) and (T4) from Table 1, respectively), and compared them with catalogued spectral classes. The result of this comparison for A5 and A7 stars is summarised in Figure 9.

Spectral class in Figure 9 is coded as follows: 3 for O3, ..., 20 for A0, ..., 40 for G0. It can be seen that spectral classes, computed from $T_{\rm eff}$ (top panel), reproduce the original data perfectly. The mean value for the histograms is 24.92 (std.dev.=1.28) for A5 stars, and 27.23 (std.dev.=1.31) for A7 stars. At the same time, spectral classes, computed from $\log g$ (bottom panel), are significantly different, on average, from the catalogued values. The histograms predict much earlier spectral classes (on

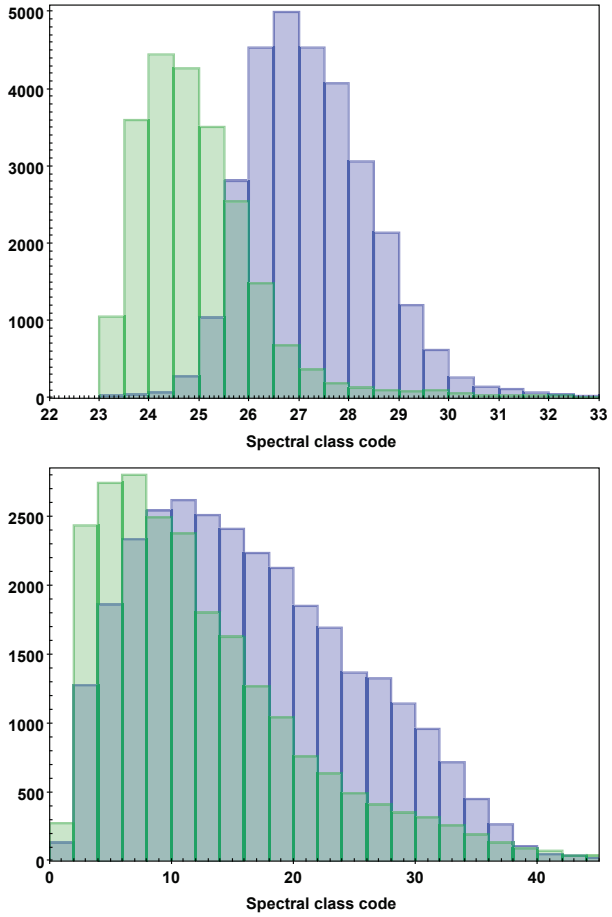

Fig. 9 Distribution of spectral class computed from $T_{\rm eff}$ (Eq. (T2), *top panel*) and $\log g$ (Eq. (T4), *bottom panel*) for 22 696 A5 stars (*green bars*) and 30 102 A7 stars (*blue bars*). The agreement of spectral classes computed from $T_{\rm eff}$ with catalogued ones is perfect, while for the $\log g$ case, the difference between the calculated and cataloged values is significant. Spectral class is coded as follows: 3 for O3, ..., 20 for A0, ..., 40 for G0.

average, B3 for the LAMOST A5 stars, and B7 for the LAMOST A7 stars), and demonstrate a much larger value spread (std.dev. values are 8.75 and 8.94, respectively). It can be suggested that LAMOST's spectral classes and $T_{\rm eff}$ values are self-consistent for MS stars, while $\log g$ values demonstrate disagreement, at least for some stars.

6 CONCLUSIONS

We have approximated spectral class – atmospheric parameters relations for MS, giant and supergiant stars, considering both observational data and published calibration tables. To judge our results, we compare them with previous representations. It appears that the agreement is satisfactory. In some regions, our results deviate from the previous data. This is a consequence of our inclusion of newer data that were not available at the time the earlier interpolation tables were compiled.

We have verified the relations for giants and MS stars with LAMOST spectral data, and the results of the comparison of our estimations with observations had been quite satisfactory. Here we consider our relations to be a formal, rough tool for spectral class estimation, so we do not apply basic laws of statistics (such as the Cromwell rule), i.e., we do not estimate the probability of the correctness of the decision.

The obtained results can be advantageous for estimation of effective temperature and surface gravity from MK spectral class or for estimation of MK spectral class from effective temperature, surface gravity and metallicity. In particular, it could help to apply SEDs from theoretical stellar atlases for given ($T_{\rm eff}$, $\log g$, [Fe/H]) values, and assign the resulting values to corresponding spectral classes. That procedure is necessary, e.g., for estimation of absolute stellar magnitudes in one or the other photometric systems implemented in modern sky surveys. It should be noted also that the use of MK spectral classification provides us with an easy (and less time-consuming) way to estimate the parameters of stars, in contrast to the ($T_{\rm eff}$, $\log g$) – model selection.

Acknowledgements We are grateful to Eric Mamajek for helpful comments and to our reviewer whose constructive comments that greatly helped us to improve the paper. OM thanks the CAS President's International Fellowship Initiative (PIFI). This work has been partially supported by NSFC/RFBR grant 20-52-53009. Guoshoujing Telescope (the Large Sky Area Multi-Object Fiber Spectroscopic Telescope, LAMOST) is a National Major Scientific Project built by the Chinese Academy of Sciences. Funding for the project has been provided by the National Development and Reform Commission. LAMOST is operated and managed by the National Astronomical Observatories, Chinese Academy of Sciences. This research has made use of the SIMBAD database, operated at CDS, Strasbourg, France, and NASA's Astrophysics Data System. This research made use of TOPCAT, an interactive graphical viewer and editor for tabular data (Taylor 2005). The acknowledgements were compiled using the Astronomy Acknowledgement Generator.

References

Allen, C. W. 1976, Astrophysical Quantities (London: Athlone (3rd edition))

Andersen, J. 1991, A&A Rev., 3, 91

Castelli, F., & Kurucz, R. L. 2003, in IAU Symposium, 210, Modelling of Stellar Atmospheres, eds. N. Piskunov, W. W. Weiss, & D. F. Gray, A20

Covey, K. R., Ivezić, Ž., Schlegel, D., et al. 2007, AJ, 134, 2398
Cui, X.-Q., Zhao, Y.-H., Chu, Y.-Q., et al. 2012, RAA (Research in Astronomy and Astrophysics), 12, 1197
de Jager, C., & Nieuwenhuijzen, H. 1987, A&A, 177, 217
Eker, Z., Bakıs, V., Bilir, S., et al. 2018, MNRAS, 479, 5491
Falcón-Barroso, J., Sánchez-Blázquez, P., Vazdekis, A., et al. 2011, A&A, 532, A95
Findeisen, K., & Hillenbrand, L. 2010, AJ, 139, 1338
Findeisen, K., Hillenbrand, L., & Soderblom, D. 2011, AJ, 142, 23
Gustafsson, B., Edvardsson, B., Eriksson, K., et al. 2008, A&A, 486, 951
Harmanec, P. 1988, Bulletin of the Astronomical Institutes of Czechoslovakia, 39, 329
Hoffleit, D., & Jaschek, C. 1991, The Bright Star Catalogue (New Haven, Conn.: Yale University Observatory, c1991, 5th rev.ed.)
Johnson, H. L. 1966, ARA&A, 4, 193
Kim, C., & Moon, B. K. 2011, AJ, 141, 118
Kim, C., & Moon, B. K. 2014, Ap&SS, 351, 229
Kraus, A. L., & Hillenbrand, L. A. 2007, AJ, 134, 2340
Le Borgne, J. F., Bruzual, G., Pelló, R., et al. 2003, A&A, 402, 433
Lejeune, T., Cuisinier, F., & Buser, R. 1997, A&AS, 125, 229
Luo, A. L., Zhao, Y.-H., Zhao, G., et al. 2015, RAA (Research in Astronomy and Astrophysics), 15, 1095
Malkov, O. Y., Sichevskij, S. G., & Kovaleva, D. A. 2010, MNRAS, 401, 695
Malkov, O., Karpov, S., Kilpio, E., et al. 2018a, Open Astronomy, 27, 62
Malkov, O., Karpov, S., Kovaleva, D., et al. 2018b, Galaxies, 7, 7
Pecaut, M. J., & Mamajek, E. E. 2013, ApJS, 208, 9
Pecaut, M. J., Mamajek, E. E., & Bubar, E. J. 2012, ApJ, 746, 154
Popper, D. M. 1980, ARA&A, 18, 115
Prugniel, P., Soubiran, C., Koleva, M., & Le Borgne, D. 2007, arXiv e-prints, astro
Sichevskij, S. G., Mironov, A. V., & Malkov, O. Y. 2014, Astrophysical Bulletin, 69, 160
Sichevskiy, S. G., Mironov, A. V., & Malkov, O. Y. 2013, Astronomische Nachrichten, 334, 832
Skiff, B. A. 2014, VizieR Online Data Catalog, B/mk
Smalley, B., & Dworetsky, M. M. 1995, A&A, 293, 446
Straižys, V. 1992, Multicolor Stellar Photometry (Tucson: Pachart Pub. House)
Taylor, M. B. 2005, TOPCAT & STIL: Starlink Table/VOTable Processing Software, in Astronomical Society of the Pacific Conference Series, 347, Astronomical Data Analysis Software and Systems XIV, eds. P. Shopbell, M. Britton, & R. Ebert, 29
Torres, G., Andersen, J., & Giménez, A. 2010, A&A Rev., 18, 67
Valdes, F., Gupta, R., Rose, J. A., Singh, H. P., & Bell, D. J. 2004, ApJS, 152, 251
Wei, P., Luo, A., Li, Y., et al. 2014, AJ, 147, 101
Zhao, G., Zhao, Y.-H., Chu, Y.-Q., Jing, Y.-P., & Deng, L.-C. 2012, RAA (Research in Astronomy and Astrophysics), 12, 723